JOC Article

Aggregation and Reactivity of the Cesium Enolate of 6-Phenyl-α-tetralone: Comparison with the Lithium Enolate[1]

Daniel Zerong Wang[†] and Andrew Streitwieser*

Department of Chemistry, University of California Berkeley, Berkeley, California 94720-1460

astreit@socrates.berkeley.edu

Received April 28, 2003

The cesium enolate of 6-phenyl-α-tetralone (CsPAT) has a λ_{max} in THF at about 387 nm, but the variation with concentration is too small for application of singular value decomposition. Proton-transfer studies with several indicators show that CsPAT forms monomer−tetramer mixtures with a tetramerization equilibrium constant, $K_{1,4} = 2.3 \times 10^{11}$ M^{-3}. The pK of the monomer is 23.39 on a scale where fluorene is assigned 22.9 (per hydrogen). For comparison, the lithium enolate, LiPAT, is also a monomer−tetramer with $K_{1,4} = 4.7 \times 10^{10}$ M^{-3} and a monomer pK = 14.22. HMPA in large amounts promotes dissociation to monomer with both enolates. Ion-pair S_N2 initial rates were measured for CsPAT with several alkyl halides and with methyl tosylate and compared with other rates with LiPAT. In all cases, the enolate monomers are much more reactive than the aggregates. Reaction of CsPAT with alkyl halides is generally C-alkylation but HMPA promotes increasing amounts of O-alkylation. A new indicator, 11-methyl-11*H*-benzo[*b*]fluorene, has a pK on the cesium scale of 23.39.

In recent papers, we have described the aggregation and reactivity of the lithium and cesium enolates of several ketones: *p*-phenylisobutyrophenone, LiPhIBP[2] and CsPhIBP,[3] 2-phenylcyclohexanone, LiPCH and CsPCH,[4] 2-(*p*-biphenylyl)cyclohexanone, LiBPCH[5] and CsBPCH,[6] 2,6-diphenyl-α-tetralone, LiPhPAT and CsPhPAT,[7] and the lithium enolates of *p*-phenylsulfonylisobutyrophenone, LiSIBP,[8] 6-phenyl-α-tetralone, LiPAT, and 2-benzyl-6-phenyl-α-tetralone, LiBnPAT.[9] In the present paper, we extend the study to the cesium enolate, CsPAT, of 6-phenyl-α-tetralone, PAT. This system was chosen because it has a close relationship to *p*-phenylisobutyrophenone, PhIBP; in both, the enolate function is not conjugated to the ring but the *p*-phenyl group provides a sufficient chromophore for UV−vis spectral study. In the tetralone system, however, the enolate function is in a conformationally fixed ring compared to the greater mobility in LiPhIBP and CsPhIBP. Moreover, the carbonyl α-position in PAT is secondary rather than tertiary as in PhIBP and permits comparisons with α-substituents. The object is a better quantitative understanding of the effect of the steric environment of the enolate on its aggregation and reactivity. The present study supplements our previous report on the aggregation and reactivity of the corresponding lithium enolate, LiPAT.[9] and additional kinetic studies are compared. For comparison, Jackman and Bortiatynski[10] have reported that the lithium salt of α-tetralone is predominantly tetrameric in THF based on NMR analysis.

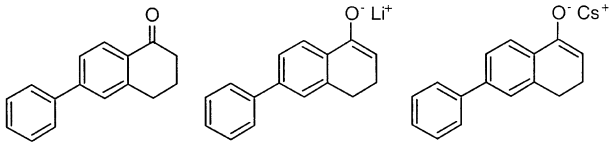

PAT LiPAT CsPAT

Alkali enolates had been well-known to be aggregated in THF solution before our work[10−13] but the equilibrium constants for aggregate formation were unknown and little was known about the relative roles of monomer and aggregates in reactions. We have shown that in alkylation reactions of all of the enolates that we have studied the second-order rate constants for the monomers are greater than for the corresponding aggregates. In the

[†] Current address: School of Science and Computer Engineering, University of Houston Clear Lake, Houston, TX 77058. E-mail: wang@cl.uh.edu.

(1) Carbon Acidity. 119.

(2) Abbotto, A.; Leung, S. S.-W.; Streitwieser, A.; Kilway, K. V. *J. Am. Chem. Soc.* **1998**, *120*, 10807−10813.
(3) Streitwieser, A.; Krom, J. A.; Kilway, K. A.; Abbotto, A. *J. Am. Chem. Soc.* **1998**, *120*, 10801−10806.
(4) Wang, D. Z.-R.; Streitwieser, A. *Can. J. Chem.* **1999**, *77*, 654−658.
(5) Streitwieser, A.; Wang, D. Z. *J. Am. Chem. Soc.* **1999**, *121*, 6213−6219.
(6) Streitwieser, A.; Wang, D. Z.-R.; Stratakis, M. *J. Org. Chem.* **1999**, *64*, 4860−4864.
(7) Wang, D. Z.-R.; Kim, Y.-J.; Streitwieser, A. *J. Am. Chem. Soc.* **2000**, *122*, 10754−10760.
(8) Abu-Hasanayn, F.; Stratakis, M.; Streitwieser, A. *J. Org. Chem.* **1995**, *60*, 4688−4689.
(9) Streitwieser, A.; Kim, Y.-J.; Wang, D. Z.-R. *Org. Lett.* **2001**, *3*, 2599−2601.
(10) Jackman, L. M.; Bortiatynski, J. *Adv. Carbanion Chem* **1992**, *1*, 45−87.
(11) Jackman, L. M.; Lange, B. C. *Tetrahedron* **1977**, *33*, 2737−2769.
(12) Bauer, W.; Seebach, D. *Helv. Chim. Acta* **1984**, *67*, 1972−1988.
(13) Seebach, D. *Angew. Chem., Int. Ed. Engl.* **1988**, *27*, 1624−1654. Heathcock, C. H. In *Comprehensive Synthetic Chemistry*; Trost, B., Ed.; Pergamon Press: New York, 1991; pp 181−238.

10.1021/jo034543d CCC: $25.00
Published on Web 10/15/2003

present work, a further objective was to learn more about the effect of enolate structure on reactivity.

We have used two complementary methods for determining the stoichiometry and equilibrium constants for aggregation of alkali enolates, the effect of concentration on the UV−vis spectra, and the use of *coupled equilibria*, usually the effect of aggregation on proton-transfer equilibria.

Spectra and p*K* of CsPAT

Solutions of CsPAT were prepared by deprotonating the ketone with diphenylmethylcesium and UV−vis spectra were taken on the solutions after successive dilutions with THF. A series of five runs were carried out in 1 mm cells, and two runs were made at higher dilution in 1 cm cells. One of the latter runs gave results inconsistent with the others and was discarded. Results of the other six runs are summarized in Table S1 (Supporting Information). Within any given run, the λ_{max} varied by a few nanometers but the normalized spectra show an isosbestic point at 387 nm. A plot of the absorbance divided by cell path length at the isosbestic point vs the formal concentration of CsPAT is linear over a concentration range of more than 2 orders of magnitude to give $\epsilon = 6627 \pm 8$ as shown in Figure S2 (Supporting Information).

The variation in λ_{max} is too small for application of singular value decomposition, an analysis applied in several previous examples of enolate aggregation.[2,4−6] Thus, we could use only the method of coupled equilibria for determining the aggregation equilibrium constants; however, the presence of an isosbestic point for CsPAT shows that only two components are present. A similar isosbestic point had been found for LiPAT. The stoichiometry and equilibrium constants for aggregate formation were determined by the effect of concentration on proton-transfer equilibria of the type in eq 1 whose observed equilibrium constant is given by eq 2.

$$RH + M^+ In^- \rightleftarrows R^- M^+ + In\ H \qquad (1)$$

$$K_{ob} = \frac{\{R^- M^+\}[In\ H]}{[RH]\{M^+ In^-\}} \qquad (2)$$

In eq 2, $\{R^- M^+\}$ denotes the formal concentration of the metal enolate. The indicators were cesium salts of highly delocalized carbanions whose relative ion pair acidities are referenced for convenience to the ionic acidity of fluorene in DMSO, pK = 22.9 per hydrogen.[14] Extensive tables of p*K*s are available for cesium salts of various indicators in THF.[15] In the present work, the cesium pK of CsPAT was measured against 11*H*-benzo[*b*]fluorene (2,3-benzofluorene, 23BF, pK = 23.63) and 9*H*-benzo[*def*]fluorene (4,5-methylenephenanthrene, 45MP, pK = 22.91).[15] In addition, in this work the pK of another indicator, 11-methyl-11*H*-benzo[*b*]fluorene (methyl-2,3-benzfluorene, Me23BF), was determined and used for a further comparison of CsPAT. The use of indicators with tertiary acidic protons is particularly convenient because they do not react significantly with the ketones studied under these conditions.

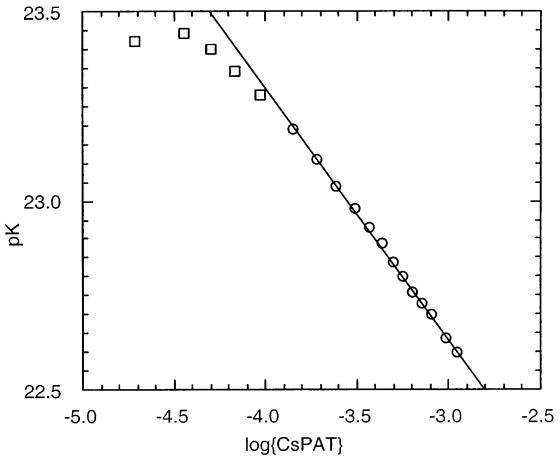

FIGURE 1. Observed pK of PAT vs the indicator Me23BF. The slope of the linear section shown (circles) is −0.663 corresponding to an average aggregation number $\tilde{n} = 2.98$.

The cesium salt of Me23BF has three absorption maxima at 692.5 (ϵ = 1272), 634.5 (ϵ = 1652), and 431.0 nm (ϵ = 23 909). The data for three runs are given in Table S2 (Supporting Information) and Lambert−Beer's Law plots leading to the ϵ values are shown in Figure S2 (Supporting Information). The pK of Me23BF on the cesium scale in THF was measured relative to 45MP; two runs with a total of 25 measurements gave pK = 23.39 ± 0.01.

A typical plot of the observed pK vs log{CsPAT} is shown in Figure 1 with Me23BF as the indicator. The slope of the linear portion, at concentrations greater than $\{CsPAT\} = 10^{-4}$ M, −0.663, corresponds to an average aggregation number of 3.0.[16] Similar plots for the other four runs are given as Figures S3−S5 (Supporting Information). These runs give average aggregation numbers of 2.95 to 3.21 and suggest that CsPAT is a mixture of mostly tetramer at these concentrations.

We have shown that for a monomer−tetramer mixture a convenient analysis of the data is to plot K_{obs} with an indicator vs the quantity $(\{CsPAT\}/K_{obs})^3$. A monomer−tetramer mixture gives a straight line with an intercept K_o, corresponding to the equilibrium constant with the enolate monomer, and a slope = $4K_{1,4}K_o^4$.[17] Such a plot for the results in Figure 1 is shown as Figure 2 and gives K_o = 0.97 (pK = 23.40), $K_{1,4} = 3.21 \times 10^{11}$ M^{-3}. Corresponding plots for the other runs are shown in Figures S6−S8 and give pK values of 23.43, 23.39. 23.39, 23.35 and $K_{1,4}$ values of 2.29×10^{11}, 2.43×10^{11}, 1.71×10^{11}, 1.82×10^{11}. The average values are: pK of the monomer, 23.39 ± 0.02, $K_{1,4} = (2.3 \pm 0.4) \times 10^{11}$ M^{-3}. Figure 3 shows the combined results of all of the runs with different indicators put on a common scale.

As shown in Table S1 λ_{max} at different concentrations of CsPAT in 1 mm cells varied from 372 to 379 nm. At the higher dilutions in a 1 cm cell λ_{max} ranged up to 387.5 nm. Although consistent results could not be obtained

(14) Bordwell, F. G. *Acc. Chem. Res.* **1988**, *21*, 456−463.
(15) Streitwieser, A.; Ciula, J. C.; Krom, J. A.; Thiele, G. *J. Org. Chem.* **1991**, *56*, 1074−1076.
(16) Kaufman, M. J.; Streitwieser, A., Jr. *J. Am. Chem. Soc.* **1987**, *109*, 6092−6097.
(17) Krom, J. A.; Petty, J. T.; Streitwieser, A. *J. Am. Chem. Soc.* **1993**, *115*, 8024−8030.

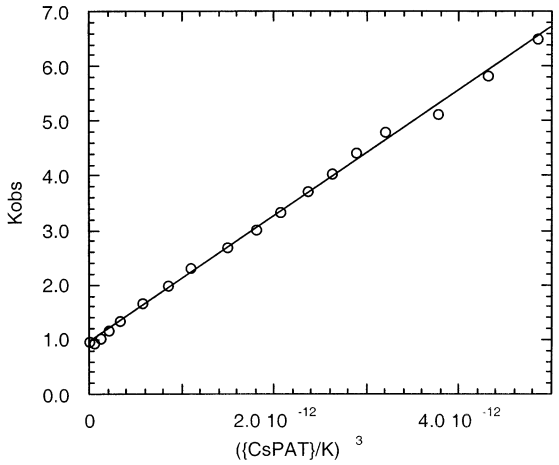

FIGURE 2. The intercept, 0.97, is K_o for the equilibrium between the monomer of CsPAT and the indicator Me23BF; the slope, 1.15×10^{12}, $= 4K_{1,4}K_o^4$.

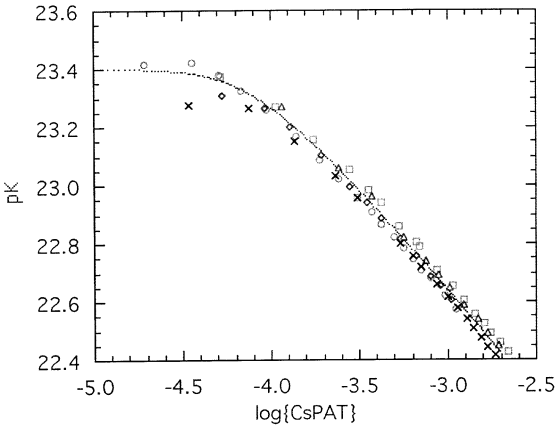

FIGURE 3. Composite of all of the pK runs of CsPAT with different indicators: circles and squares, Me23BF; diamonds and triangles, 23BF; crosses, 45MP. The dotted line is that calculated for the average values: pK of the monomer, 23.39; $K_{1,4} = 2.3 \times 10^{11}$ M^{-3}.

in applying SVD to these data, using the value determined above for $K_{1,4}$ the amounts of monomer and tetramer present in each of the solutions in Table S1 could be evaluated. Plotting the observed λ_{max} vs the mole fraction of monomer, N(monomer), in each solution gives a linear correlation with some scatter (Figure S9, Supporting Information) but extrapolation to $N = 0$ and $N = 1$ gives the λ_{max} of tetramer and monomer, 372 and 385 nm, respectively. A similar plot for LiPAT gives λ_{max} of tetramer and monomer, 340 and 347 nm, respectively, a substantially smaller difference between monomer and aggregate.

The pK of CsPAT, 23.39, is substantially higher than that of the corresponding lithium enolate, LiPAT, 14.22.[9] We emphasize again that these values are *not* pK_a but are values referred to an arbitrary (but convenient) standard. All of the cesium salts are contact ion pairs (CIP). The lithium enolate is referred to a solvent-separated ion pair (SSIP) standard; the much lower value of LiPAT relative to CsPAT indicates that, in common with all of the other lithium enolates we have studied, LiPAT is present in THF as a contact ion pair whose dissociation constant is much lower than those of the lithium indicator salts studied.[18] CsPAT is more aggregated than LiPAT whose $K_{1,4} = 4.7 \times 10^{10}$ M^{-3} but the difference in $\Delta G°$ is only 1 kcal mol^{-1}. An important driving force for dissociation of the tetramer to monomer is the resulting increased solvation of the metal cation. This principle has been shown generally for 1:1 salts,[19] and has been demonstrated not only for enolates[20] but also for lithium phenolates[21] and computationally.[22] The present results show the increased solvation of the monomeric cesium enolate is almost as great as that of lithium enolate.

This effect is also shown by the effects of HMPA, which had been shown earlier to convert lithium enolate aggregates to monomers.[23] This effect of HMPA is well-known for other lithium compounds, for example, lithium phenolates,,[24] lithiated nitriles,[25] lithium amides,[26−28] (but note)[29] lithium chloride,[30] and aryllithiums.[31−33] Small amounts of HMPA, up to 0.1 M, have little effect on the λ_{max} of CsPAT, but larger amounts, up to 1 M, cause bathochromic shifts to 385 nm (Figure S11, Supporting Information), the λ_{max} estimated above for the monomer. Thus, even the large cesium cation is sufficiently solvated by HMPA to stabilize the monomer. Similarly, HMPA causes a shift of λ_{max} of LiPAT to 353 nm (Figure S12, Supporting Information), only slightly greater than that estimated above for the monomer. These changes can be compared to the effects of HMPA on the spectra of some indicators. Addition of HMPA to the cesium salt of *p*-biphenylyldiphenylmethane causes a progressive bathochromic shift, probably a change from the contact ion pair cesium salt to increasing amounts of SSIP. However, HMPA has no effect on the spectrum of the lithium salt of trimethyldihydroanthracene, undoubtedly because this lithium salt is an SSIP to begin with.

(18) Kaufman, M. J.; Gronert, S.; Streitwieser, A., Jr. *J. Am. Chem. Soc* **1988**, *110*, 2829−2835.
(19) Chabanel, M. *Pure Appl. Chem*. **1990**, *62*, 35−46.
(20) Streitwieser, A.; Juaristi, E.; Kim, Y.-J.; Pugh, J. K. *Org. Lett.* **2000**, *2*, 3739−3741.
(21) Jackman, L. M.; DeBrosse, C. W. *J. Am. Chem. Soc.* **1983**, *105*, 4177−4184.
(22) Pratt, L. M.; Streitwieser, A. *J. Org. Chem*. **2003**, *68*, 2830−2838.
(23) Leung, S. S.-W.; Streitwieser, A. *J. Org. Chem*. **1999**, *64*, 3390−3391.
(24) Jackman, L. M.; Chen, X. *J. Am. Chem. Soc.* **1992**, *114*, 403−411.
(25) Carlier, P. R.; Lo, C. W.-S. *J. Am. Chem. Soc* **2000**, *122*, 12819−12823.
(26) Jackman, L. M.; Scarmoutzos, L. M.; Smith, B. D.; Williard, P. G. *J. Am. Chem. Soc.* **1988**, *110*, 6058−6063.
(27) Sato, D.; Kawasaki, H.; Shimada, I.; Arata, Y.; Okamura, K.; Date, T.; Koga, K. *J. Am. Chem. Soc.* **1992**, *114*, 761−763.
(28) Romesberg, F. E.; Bernstein, M. P.; Gilchrist, J. H.; Harrison, A. T.; Fuller, D. J.; Collum, D. B. *J. Am. Chem. Soc.* **1993**, *115*, 3475−3483.
(29) Romesberg, F. E.; Gilchrist, J. H.; Harrison, A. T.; Fuller, D. J.; Collum, D. B. *J. Am. Chem. Soc.* **1991**, *113*, 5751−5757.
(30) Reich, H. J.; Borst, J. P.; Dykstra, R. R. *J. Am. Chem. Soc.* **1993**, *115*, 8728−8741.
(31) Reich, H. J.; Gudmundsson, B. O. *J. Am. Chem. Soc.* **1996**, *118*, 6074−6075.
(32) Reich, H. J.; Green, D. P.; Medina, M. A.; Goldenberg, W. S.; Gudmundsson, B. O.; Dykstra, R. R.; Phillips, N. H. *J. Am. Chem. Soc.* **1998**, *120*, 7201−7210.
(33) Reich, H. J.; Goldenberg, W. S.; Gudmundsson, B. O.; Sanders, A. W.; Kulicke, K. J.; Simon, K.; Guzei, I. A. *J. Am. Chem. Soc.* **2001**, *123*, 8067−8079.

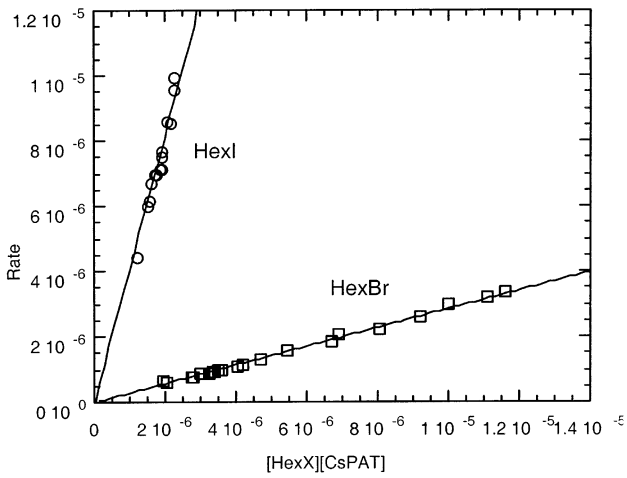

FIGURE 4. Initial rates of *n*-hexyl iodide and bromide compared to the monomer concentration of CsPAT times the concentration of RX. Slopes shown are as follows: HexI, $k_2 = 4.07 \pm 0.05$ M^{-1} s^{-1}, $R^2 = 0.933$; HexBr, $k_2 = 0.294 \pm 0.004$ M^{-1} s^{-1}, $R^2 = 0.982$.

Alkylation Kinetics

We had shown previously that the alkylation reactions of several lithium and cesium enolates occur dominantly with the enolate monomers.[2,5−9] In the present work, we include additional examples of such alkylations because these are ion-pair S_N2 reactions and it would be valuable to have examples of structural effects for comparison with ionic S_N2 reactions in more polar solvents. Earlier studies of relative reactivities of different enolates in ether are less useful for this purpose because the role of aggregation was not determined.[34−38] Lithium halides have been shown to form mixed aggregates with lithium enolates;[39,40] although such mixed aggregates have not been demonstrated for cesium salts, we followed our usual procedure of measuring initial rates. A large excess of the alkylating agent was added to a solution of the enolate in THF, and the absorbance of the enolate was followed at λ_{max}. The slope of about the first 10−15% reaction was used to determine the rate constant of the pseudo-first-order reaction using the calculated concentration of the enolate monomer. Using this slope as an approximation to the logarithm will give numbers about 5% low, but no correction was made because the experimental error is probably somewhat greater than this. Examples of the results with *n*-hexyl bromide and iodide are shown in Figure 4. The data are summarized in Tables S3 and S4 (Supporting Information). Each point is a separate kinetic run using different concentrations of enolate and/or halide. Hexyl halides were used because of volatility considerations in our glovebox system. It should be noted again that any significant reaction via an aggregate would show up as upward curvature of plots such as in Figure 4.

TABLE 1. Summary of Rate Constants

RX	k_2, M^{-1} s^{-1}
n-hexyl chloride	$(1.15 \pm 0.03) \times 10^3$
n-hexyl bromide	0.292 ± 0.004
n-hexyl iodide	4.07 ± 0.05
methyl tosylate	4.30 ± 0.09
p-*t*-Bu-benzyl chloride	0.59 ± 0.01

n-Hexyl chloride is much less reactive, and a constant concentration of enolate was used with varying excess amounts of halide. These results are summarized in Table S5 and Figure S15 (Supporting Information). Methyl tosylate was included but gave more scatter than the *n*-hexyl halides. Its results are summarized in Table S6 and Figure S16 (Supporting Information). Finally, *tert*-butylbenzyl chloride (BBC) is shown in Table S7 and Figure S17 (Supporting Information). The rate constants found are summarized in Table 1. The errors shown are the standard deviations of the linear slopes, but the true probable errors are closer to 10%.

The reactivity order of the hexyl halides is typical of S_N2 reactions.[41] In particular, the relative reactivity of the iodide is essentially normal. If its reaction involved single electron transfer a much larger rate constant would have been expected. This result agrees with that found previously for the reaction of the cesium enolate of 2,6-diphenyl-α-tetralone (CsPhPAT) with *n*-hexyl iodide.[7] Tosylates are usually somewhat more reactive than the corresponding bromides and that is found here, also in agreement with results with CsPhPAT.[7] Similarly, benzyl halides are typically 2 orders of magnitude more reactive in S_N2 reactions than ethyl halides; in the present case, BBC is 500 times more reactive than *n*-hexyl chloride and fits the typical pattern well.

Alkylation kinetics were also run with the lithium enolate, LiPAT. Results of alkylation and dialkylation with benzyl bromide were published earlier.[9] Additional runs were made with some substituted benzyl bromides and with methyl brosylate (MeOBs). In most cases, there was an initial rapid decrease in the enolate absorbance on adding the alkylating agent followed by a slower decrease. In these cases, the initial rate was determined after the first 20−30 s and following the reaction for an additional approximately 10%. This procedure is somewhat different from that used with the reaction of LiPAT with benzyl bromide reported earlier;[9] a reanalysis of this reaction gives a rate constant about 10% greater, $k_2 = 0.105$ M^{-1} s^{-1}. Results for *o*-chlorobenzyl bromide (oClBnBr) and *o*-methylbenzyl bromide (oMeBnBr) are given in Tables S8 and S9 (Supporting Information) and displayed in Figure 5. Similar results for *m*-chlorobenzyl bromide and methyl brosylate are summarized in Tables S10 and S11 and Figures S18 and S19 (Supporting Information). The rate constants are summarized in Table 2.

Earlier, we found that the reaction of MeOBs with CsPhPAT is 6.8 times that of MeOTs. If that same ratio applies to the present case, CsPAT monomer is found to be 3400 times as reactive as that of LiPAT. We had also

(34) Zook, H. D.; Rellahan, W. L. *J. Am. Chem. Soc.* **1957**, *79*, 881−886.
(35) Zook, H. D.; Gumby, W. L. *J. Am. Chem. Soc.* **1960**, *82*, 1386−1389.
(36) Zook, H. D.; Russo, T. J.; Ferrand, E. F.; Stotz, D. S. *J. Org. Chem.* **1968**, *33*, 2222−2228.
(37) Caine, D.; Huff, B. J. L. *Tetrahedron Lett.* **1966**, 4695−4700.
(38) Caine, D.; Huff, B. J. L. *Tetrahedron Lett.* **1967**, 3399−3403.
(39) Jackman, L. M.; Haddon, R. C. *J. Am. Chem. Soc.* **1973**, *95*, 3687−3692.
(40) Abu-Hasanayn, F.; Streitwieser, A. *J. Am. Chem. Soc.* **1996**, *118*, 8136−8137.
(41) Streitwieser, A. *Chem. Rev.* **1956**, *56*, 571.

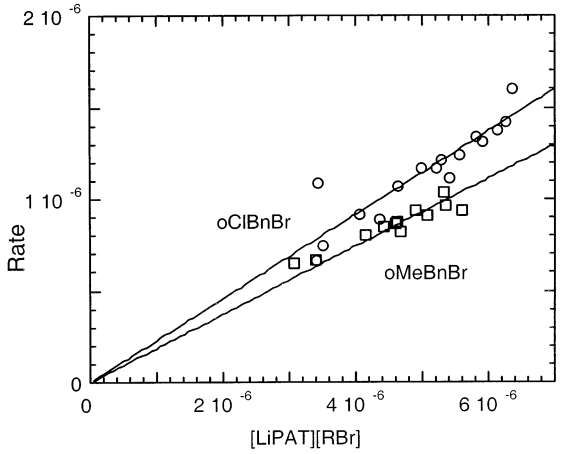

FIGURE 5. Initial rates (M^{-1} s^{-1}) of reaction of *o*-chlorobenzyl bromide (circles) and *o*-methylbenzyl bromide (squares) compared to [RBr][LiPAT monomer]. The two slopes shown are as follows: oClBnBr, $k_2 = 0.229 \pm 0.005$ ($R^2 = 0.83$), oMeBnBr, $k_2 = 0.186 \pm 0.003$ ($R^2 = 0.82$).

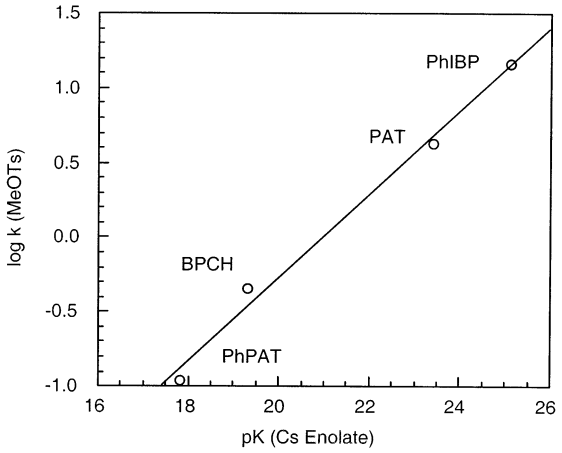

FIGURE 6. Brønsted plot of log k_2 with MeOTs of the monomer ion pair p*K*s of cesium enolates in THF at 25 °C. Points shown are as follows: PhIBP, *p*-phenylisobutyrophenone; PAT, 6-phenyl-α-tetralone; BPCH, 2-p-biphenylylcyclohexanone; PhPAT, 2,6-diphenyl-α-tetralone. Slope shown is 0.278 ± 0.019; $R^2 = 0.99$.

TABLE 2. Second-Order Rate Constants for Reaction of LiPAT Monomer with Alkylating Agents in THF at 25 °C

RX	k_2, M^{-1} s^{-1}
benzyl bromide	0.105
o-methylbenzyl bromide	0.186
o-chlorobenzyl bromide	0.229
m-chlorobenzyl bromide	0.187
methyl *p*-bromobenzenesulfonate	0.0085

shown that the rates of reaction with MeOTs of three cesium enolates correlated well with their p*K*s. We can now add CsPAT to this correlation as a fourth point and find that it also fits well (Figure 6) This relation amounts to a Brønsted plot with a slope having a relatively small value of 0.28. Thus, the effective basicity of a cesium enolate is dominant in its reactivity with MeOTs but apparently with a relatively early transition state.

The corresponding lithium enolates give no such correlation. The addition of LiPAT from the present study gives five lithium enolates whose monomer p*K*s and rates

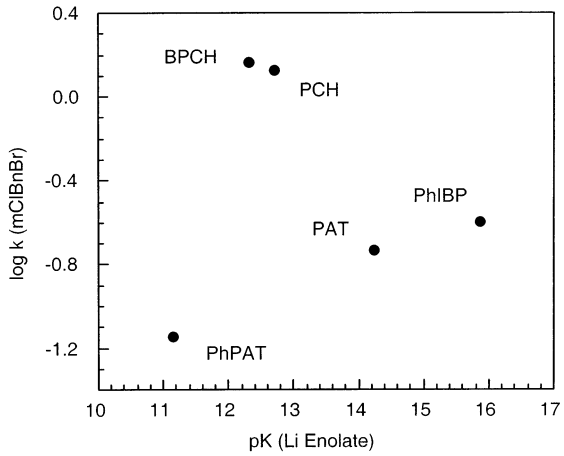

FIGURE 7. Rates of lithium enolate monomers with *m*-chlorobenzyl bromide compared to the enolate p*K*s. Points shown are as follows: BPCH, 2-p-biphenylylcyclohexanone; PCH, 2-phenylcyclohexanone; PhIBP, *p*-phenylisobutyrophenone; PAT. 6-phenyl-α-tetralone; PhPAT, 2,6-diphenyl-α-tetralone.

with mClBnBr are known. As shown in Figure 7, these data give no Brønsted correlation. Apparently, the electrophilic character of the lithium cation is as important as the basicity of the enolate; that is, these rates are dependent to an important extent on two independent properties and not just one.

In previous work, HMPA was shown to increase rates of reaction with alkylating agents not only by deaggregating enolate aggregates to monomers but also by increasing the reactivity of the monomers.[23] It was shown above that it requires about 1 M HMPA to completely deaggregrate LiPAT to the monomer. Accordingly, the reaction of LiPAT with methyl brosylate in the presence of 0.25 M HMPA is still of fractional order in {LiPAT} but is about 70-fold faster than in the absence of HMPA (Figure S20, Supporting Information). We did not obtain an accurate measure of the reactivity of CsPAT in the presence of HMPA but did find that its rate of reaction with *n*-hexyl chloride and 0.36 M HMPA is roughly 40 times faster than without HMPA.

Product Studies

In previous product studies with the cesium and lithium enolates of 2,6-diphenyl-α-tetralone, we reported that reactions with alkyl halides gave almost exclusively C-alkylation but that reactions of the cesium enolate with methyl sulfonates gave substantial amounts of O-alkylation. These observations were further extended in the present study.

PAT has two α-hydrogens and can form mono- and dialkylation products (Scheme 1). The initial O-alkylation product cannot undergo further reaction, but the product of C-alkylation can undergo further alkylation to give CC and CO dialkylation. The role of aggregation in determining the amount of dialkylation was reported recently.[9]

Reaction products were determined for a number of kinetic solutions allowed to stand for a prolonged period. Products were identified by GC−MS, and the mixtures were analyzed using the uncalibrated GC areas. Accordingly, the results will not be completely accurate but the

SCHEME 1. Mono- and Dialkylation Products

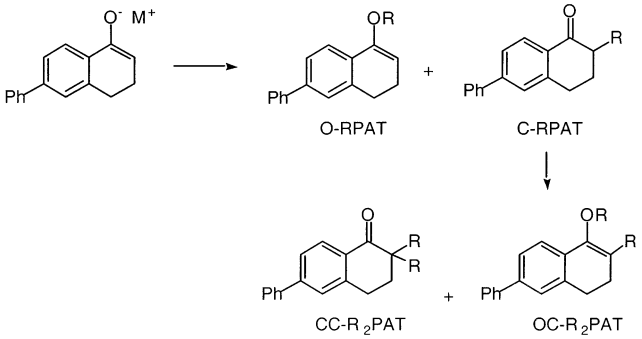

TABLE 3. C- and O-Alkylation Products of Reaction of LiPAT with *n*-Hexyl Halides

RX	HMPA, M	*f*(O)[a]	*f*(C)[b]	*f*(OC)[c]	*f*(CC)[d]	1st alk f(C)[e]	2nd alk *f*(C)[f]
HexCl	0	0.00	1.00	0.00	0.00	1.00	
HexBr		0.00	1.00	0.00	0.00	1.00	
HexI		0.00	1.00	0.00	0.00	1.00	
HexCl	0.50	0.00	1.00	0.00	0.00	1.00	1.00
HexBr		0.00	0.98	0.00	0.02	1.00	1.00
HexI		0.00	0.88	0.00	0.12	1.00	1.00
HexCl	0.99	0.00	0.98	0.00	0.02	1.00	1.00
HexBr		0.00	0.90	0.06	0.04	1.00	0.41
HexI		0.00	0.78	0.06	0.17	1.00	0.75
HexCl	1.54	0.00	0.98	0.00	0.02	1.00	1.00
HexBr		0.00	0.86	0.08	0.05	1.00	0.39
HexI		0.00	0.85	0.05	0.10	1.00	0.68
HexCl	1.99	0.00	0.97	0.00	0.03	1.00	1.00
HexBr		0.00	0.89	0.07	0.04	1.00	0.34
HexI		0.00	0.85	0.05	0.10	1.00	0.66
HexCl	2.98	0.00	0.91	0.08	0.02	1.00	0.18
HexBr		0.00	0.88	0.09	0.03	1.00	0.27
HexI		0.00	0.85	0.05	0.09	1.00	0.65
HexCl	3.96	0.00	0.87	0.11	0.02	1.00	0.13
HexBr		0.00	0.87	0.10	0.03	1.00	0.25
HexI		0.00	0.84	0.05	0.10	1.00	0.65
HexCl	4.88	0.00	0.89	0.10	0.01	1.00	0.11
HexBr		0.00	0.91	0.08	0.01	1.00	0.15
HexI		0.00	0.92	0.03	0.05	1.00	0.57
HexCl	5.69	0.07	0.85	0.04	0.03	0.93	0.43
HexBr		0.34	0.62	0.04	0.00	0.66	0.00
HexI		0.00	0.81	0.07	0.12	1.00	0.62

[a] O-RPAT/total area of four products. [b] C-RPAT/total area of four products. [c] OC-R_2PAT/total area of four products. [d] CC-R_2PAT/total area of four products. [e] Fraction of C-alkylation for the first alkylation = C-RPAT + OC-R_2PAT + CC-R_2PAT/total area of four products. [f] Fraction of C-alkylation for the second alkylation = CC-R_2PAT/(OC-R_2PAT + CC-R_2PAT).

trends are clear. Tables 3 and 4 give the results for alkylation of LiPAT and CsPAT, respectively, with the *n*-hexyl halides in the presence and absence of HMPA. As mentioned above, the O-alkylation product, O-RPAT, cannot undergo further reaction, but the C-alkylation product can undergo further alkylation to give both CC- and OC-dialkylation products. Thus, for the first alkylation, the relative amount of C-alkylation is determined by the sum of C-RPAT and the dialkylation products. The results in Table 3 show that LiPAT gives exclusively C-alkylation with the hexyl halides. Small amounts of HMPA do not change this result although with HMPA, the second alkylation is increasingly at oxygen. Only at the highest amount of HMPA used, 5.69 M, is significant O-alkylation found for the first alkylation. But the amounts of O-alkylation are generally small and trends among the different halides are not consistent.

TABLE 4. C- and O-Alkylation Products of Reaction of CsPAT with *n*-Hexyl Halides

RX	HMPA, M	*f*(O)[a]	*f*(C)[b]	*f*(OC)[c]	*f*(CC)[d]	1st alk *f*(C)[e]	2nd alk *f*(C)[f]
HexCl	0.0	0.29	0.26	0.26	0.19	0.71	0.42
HexBr		0.11	0.26	0.36	0.27	0.89	0.43
HexI		0.10	0.36	0.23	0.31	0.90	0.58
HexCl	0.50	0.73	0.07	0.19	0.01	0.27	0.04
HexBr		0.52	0.14	0.28	0.05	0.48	0.15
HexI		0.18	0.40	0.25	0.18	0.82	0.43
HexCl	1.00	0.81	0.02	0.16	0.00	0.19	0.03
HexBr		0.62	0.09	0.27	0.03	0.38	0.10
HexI		0.24	0.35	0.26	0.15	0.76	0.37
HexCl	1.42	0.85	0.01	0.14	0.00	0.15	0.00
HexBr		0.65	0.12	0.22	0.02	0.35	0.07
HexI		0.29	0.46	0.17	0.08	0.71	0.31
HexCl	1.89	0.87	0.01	0.12	0.00	0.13	0.00
HexBr		0.69	0.12	0.19	0.00	0.31	0.00
HexI		0.35	0.47	0.14	0.03	0.65	0.18
HexCl	2.83	0.87	0.03	0.10	0.00	0.13	0.00
HexBr		0.69	0.14	0.17	0.00	0.31	0.00
HexI		0.32	0.51	0.13	0.04	0.68	0.22
HexCl	4.02	0.92	0.01	0.07	0.00	0.08	0.00
HexBr		0.75	0.13	0.12	0.00	0.25	0.00
HexI		0.39	0.52	0.09	0.00	0.61	0.00
HexCl	4.78	0.94	0.03	0.02	0.00	0.06	0.00
HexBr		0.75	0.17	0.09	0.00	0.25	0.00
HexI		0.39	0.54	0.07	0.00	0.61	0.00
HexCl	5.69	0.84	0.04	0.11	0.00	0.16	0.00
HexBr		0.77	0.01	0.20	0.02	0.23	0.08
HexI		0.36	0.44	0.14	0.05	0.64	0.27

[a] O-RPAT/total area of four products. [b] C-RPAT/total area of four products. [c] CO-R_2PAT/total area of four products. [d] CC-R_2PAT/total area of four products. [e] Fraction of C-alkylation for the first alkylation = C-RPAT + OC-R_2PAT + CC-R_2PAT/total area of four products [f] Fraction of C-alkylation for the second alkylation = CC-R_2PAT/(OC-R_2PAT + CC-R_2PAT).

The results with CsPAT in Table 4 are significantly different. Even without HMPA, CsPAT gives substantial O-alkylation, but again, the second alkylation is still greater on oxygen. With addition of even small amounts of HMPA, the extent of O-alkylation is increased. O-Alkylation is also more important for RCl than for RI with RBr being intermediate. In the reaction of CsPAT with *p*-*tert*-butylbenzyl chloride, only the mono- and dialkylation products of C-alkylation were found and identified.

These results on C- vs O-alkylation agree well with the generalizations summarized by le Noble several decades ago.[42]

Conclusions

CsPAT forms monomer−tetramer mixtures in THF as does LiPAT. Aggregation of an ion pair is electrostatically favorable but the driving force is reduced for large cations such as cesium compared to lithium. Solvation of the cation preferentially stabilizes the monomer and such solvation is more important for lithium than for the larger cesium. These two opposing effects are apparently of comparable importance for these enolates in THF because the tetramerization equilibrium constant for CsPAT is only slightly greater than for LiPAT. Solvation of the cesium cation in CsPAT is still important as shown by the effect of HMPA which shifts the equilibrium toward monomer as it does for LiPAT.

(42) le Noble, W. *Synthesis* **1970**, 1−6.

In alkylation reactions, the monomer of CsPAT is much more reactive than the tetramer. The *n*-hexyl halides show a normal reactivity order: RI > RBr > RCl. Methyl tosylate is about as reactive as *n*-hexyl iodide and *p-tert*-butylbenzyl chloride is twice as reactive as *n*-hexyl bromide. The monomer of CsPAT is about 3000 times more reactive than the monomer of LiPAT. Together with several other cesium enolates, the reaction of CsPAT with methyl tosylate gives a Brønsted correlation of log *k* vs p*K*, indicating that the basicity of the enolate moiety is an important driving force in this alkylation. However, the relatively small Brønsted slope of 0.28 suggests an early transition state. Lithium enolates give no such Brønsted correlation suggesting that the electrophilic character of the lithium cation in the transition state (or some other independent property) is of comparable importance to the nucleophilicity of the enolate group. These observations have additional significance since these are ion pair S_N2 reactions instead of the more traditional reactions with anions.

The alkylation reactions of LiPAT with alkyl halides are exclusively those of C-alkylation. Only with the addition of large amounts of HMPA does O-alkylation compete. This observation suggests that alkylation reactions of lithium enolates could be enhanced by adding HMPA with little danger of loss to O-alkylation. CsPAT, however, gives substantial O-alkylation even in the absence of HMPA. Addition of HMPA further increases the role of O-alkylation. Coordination of the enolate oxygen clearly favors C-alkylation. Weakening this interaction, either by using a large cation or by making the cation effectively larger with solvation, enhances the role of O-alkylation. Increased steric hindrance at the carbon center, however, such as by a substituent, also enhances O-alkylation.

Experimental Section

All UV measurements were carried out in a glovebox under argon atmosphere at a constant temperature of 25.0 ± 0.1 °C, maintained by a cooling bath. The sample compartment located in the floor of the glovebox was connected to a Shimadzu 3801 spectrometer with fiber optic cables. THF was purified as described previously.[43] Most indicators were available from previous work. The alkylating agents and indicators were purified by vacuum sublimation or distillation. The preparation of PAT was described previously.[7]

11-Methyl-11*H*-benzo[*b*]fluorene. This hydrocarbon has been reported in the literature but without characterization.[44] To a solution of 4.33 g of benzo[*b*]fluorenone[45] in 400 mL of dry ether was added 10 mL of 3.0 M methylmagnesium bromide. The solution was refluxed and quenched with HCl, and the product was extracted with ether. Removal of solvent from the washed and dried extract gave 4.98 g of 7-methyl-7*H*-benzo[*b*]fluoren-7-ol. This material was reduced with HI/AcOH because in other work we found that hydrogenolysis of carbinols containing a naphthalene ring gave some reduction at naphthalene to give impurities difficult to remove. The above carbinol was refluxed with 40 mL of HI in 240 mL of acetic acid until reaction was completed as indicated by TLC. The product was extracted with ether, washed, dried, and distilled. Purification by column chromatography (hexane/ethyl acetate = 50:1), and sublimation under vacuum gave 0.98 g of pure compound (23% yield): mp 116−118 °C; ^{1}H NMR (300 MHz, $CDCl_3$) δ 8.19 (s, 1H), 7.87 (m, 4H), 7.54−7.57 (m, 1H), 7.36−7.52 (overlapping multiplets, 4H), 4.16 (q, J = 7.5 Hz, 1H), 1.64 (d, J = 7.5 Hz, 3H); ^{13}C NMR (400 MHz, $CDCl_3$) δ 149.5, 147.2, 140.0, 139.5, 133.2, 128.2, 127.9, 127.8, 127.2, 125.5, 125.4, 124.3, 122.5, 120.6, 117.9, 71.2, 42.0, 19.3. Anal.[46] Calcd for $C_{18}H_{14}$: C, 93.87; H, 6.13. Found: C, 93.73; H, 6.07.[47]

Reaction Product: CsPAT + *n*-Hexyl Bromide. Products were separated by preparative TLC. O-Alkylation product (4-hexyloxy-7-phenyl-1,2-dihydronaphthalene): ^{1}H NMR ($CDCl_3$, 300 MHz) δ 8.11 (d, J = 8.19 Hz, 1H), 7.61 (d, J = 7.6 Hz, 2H), 7.54−7.46 (m, 3H), 7.43−7.36 (m, 3H), 3.02 (t, J = 6.3 Hz, 2H), 2.09−2.05 (m, 2H), 1.69−1.66 (m, 2H), 1.34−1.26 (m, 8H), 0.85 (t, J = 6.8 Hz, 3H); MS (*m*/*z*, rel intensity) 308 (4), 307 (23), 306 (100), 305 (3), 236 (7), 235 (34), 222 (5), 221 (3), 207 (6), 194 (8), 165 (7). C-Alkylation product (2-hexyl-6-phenyl-α-tetralone): ^{1}H NMR ($CDCl_3$ 300 MHz) δ 8.10 (d, J = 8.15 Hz), 1H), 7.63−7.51 (m, 2H), 7.49−7.30 (m, 4H), 7.28−7.17 (m, 1H), 3.12−3.02 (m, 1H), 2.54−2.46 (m, 1H), 2.32−2.23 (m, 1H), 2.00−1.82 (m, 2H), 1.58−1.26 (m, 10H), 0.97−0.87 (m, 3H); MS (*m*/*z*, rel intensity) 307 (3), 306 (31), 222 (100), 221 (14), 207 (8), 194 (5), 166 (8), 165 (18).

Reaction Product: CsPAT + *p-tert*-Butylbenzyl Chloride. Monoalkylated (2-(*p-tert*-butylbenzyl)-6-phenyl-α-tetralone): MS (*m*/*z*, rel intensity) 370 (4), 369 (28), 368 (100), 367 (45), 353 (20), 320 (6), 311 (4), 234 (5), 222 (3), 221 (17), 194 (5), 193 (4), 178 (3), 165 (9). Dialkylated product (2,2-bis(*p-tert*-butylbenzyl)-6-phenyl-α-tetralone: MS (*m*/*z*, rel intensity) 514 (1), 499 (1), 369 (7), 368 (41), 367 (100), 353 (3), 311 (4), 310 (1), 295 (6), 294 (22), 221 (3); HRMS found 515.3324, calcd 515.3314.

Acknowledgment. This work was supported in part by NSF Grant No. 9980367.

Supporting Information Available: Experimental details (12 tables and 20 figures). This material is available free of charge via the Internet at http://pubs.acs.org.

JO034543D

(43) Gronert, S.; Streitwieser, A., Jr. *J. Am. Chem. Soc.* **1986**, *108*, 7016−7022.
(44) Lavoie, E. J.; Tulley, L.; Bedenko, V.; Hoffmann, D. *Mutat. Res.* **1981**, *91*, 167−176.
(45) Streitwieser, A.; Brown, S. M. *J. Org. Chem.* **1988**, *53*, 904−906.
(46) Analysis by Analytical Services Laboratory, University of California, Berkeley.
(47) Characterizations by Dr. Arlene McKeown.